Biochimica et Biophysica Acta 1797 (2010) 189–196

Contents lists available at ScienceDirect

Biochimica et Biophysica Acta

journal homepage: www.elsevier.com/locate/bbabio

Impact of mitochondriotropic quercetin derivatives on mitochondria

Lucia Biasutto [a,b], Nicola Sassi [a], Andrea Mattarei [b], Ester Marotta [b], Paola Cattelan [c], Antonio Toninello [c], Spiridione Garbisa [a], Mario Zoratti [a,d,*], Cristina Paradisi [b]

[a] Department of Biomedical Sciences, University of Padova, Padova, Italy
[b] Department of Chemical Sciences, University of Padova, Padova, Italy
[c] Department of Biological Chemistry, University of Padova, Padova, Italy
[d] CNR Institute of Neuroscience, Padova, Italy

ARTICLE INFO

Article history:
Received 7 August 2009
Received in revised form 18 September 2009
Accepted 7 October 2009
Available online 14 October 2009

Keywords:
Mitochondrial permeability transition
Mitochondria-targeted polyphenol
Reactive oxygen species
Transmembrane potential
Uncoupling

ABSTRACT

Mitochondria-targeted polyphenols are being developed with the intent to intervene on the levels of reactive oxygen species (ROS) in mitochondria. Polyphenols being more than just anti-oxidants, the interaction of these derivatives with the organelles needs to be characterised. We have studied the effects of two quercetin derivatives, 3-(4-O-triphenylphosphoniumbutyl)quercetin iodide (Q3BTPI) and its tetracetylated analogue (QTA3BTPI), on the inner membrane aspecific permeability, transmembrane voltage difference and respiration of isolated rat liver mitochondria. While the effects of low concentrations were too small to be reliably defined, when used in the 5–20 μM range these compounds acted as inducers of the mitochondrial permeability transition (MPT), an effect due to pro-oxidant activity. Furthermore, Q3BTPI behaved as an uncoupler of isolated mitochondria, causing depolarisation and stimulating oxygen consumption. When applied to tetramethylrhodamine methyl ester (TMRM)-loaded HepG2 or Jurkat cells uptake of the compounds was predictably associated with a loss of TMRM fluorescence, but there was no indication of MPT induction. A production of superoxide could be detected in some cells upon prolonged incubation of MitoSOX®-loaded cells with QTA3BTPI. The overall effects of these model mitochondriotropic polyphenols may thus differ considerably depending on whether their hydroxyls are protected or not and on the experimental system. *In vivo* assays will be needed for a definitive assessment of their bioactivities.

1. Introduction

The production of Reactive Oxygen Species (ROS) in cells, and in particular by mitochondria, is considered to be a major factor in aging and degenerative processes (e.g.: [1–5]) with the implication that undesirable organism deterioration may be slowed down by anti-oxidants. Anti-oxidants, including polyphenols, are thus included in some cosmetics and nutritional supplements. In ischemia/reperfusion (I/R) injury, much of the damage is sustained when circulation is reinstated. A major role in cell death under these circumstances is played by the Mitochondrial Permeability Transition (MPT), a process induced by matrix Ca^{2+} overload and oxidative conditions [6–8]. The involvement of ROS in MPT induction is clearly recognised (e.g.: [2,9,10], and antioxidants may be expected to exert a protective effect. This has led to an ongoing effort to develop "mitochondriotropic" antioxidants [11–18], including polyphenols [19,20], mainly with the goal of counteracting these undesirable redox-mediated effects. However, μM concentrations of mitochondria-targeted quercetin and resveratrol derivatives proved to be cytotoxic for rapidly dividing cultured cells [19,20], suggesting a potential as chemotherapeutic agents. Understanding the reasons for this cytotoxicity ought to help the design of other mitochondria-targeted antioxidants and the utilisation of already available ones.

It is therefore important to characterise the effects of these mitochondria-targeted compounds on isolated mitochondria and on the organelles in cells to gain a sense of what may happen *in vivo*. Here we report our observations with isolated rat liver mitochondria (RLM), cultured HepG2 and Jurkat cells, and two mitochondria-

Abbreviations: BC, Bathocuproinedisulfonic acid; BF, Bathofenanthrolinedisulfonic acid; BHT, 2,5-di-t-Butyl-p-HydroxyToluene; CsA, Cyclosporine A; DTT, Dithiothreitol (1,4-Dimercapto-2,3-butanediol); $\Delta\tilde{\mu}_H$, transmembrane electrochemical proton gradient; $\Delta\Psi$, mitochondrial transmembrane electrical potential difference; FCCP, carbonyl cyanide p-trifluorometoxyphenyl hydrazone; IMM, Inner Mitochondrial Membrane; HE, diHydroEthidine; HBSS, Hank's Balanced Salt Solution; LC/MS, Liquid Chromatography / Mass Spectrometry; MPT, Mitochondrial Permeability Transition; RLM, Rat liver Mitochondria; ROI, Region of Interest; ROS, Reactive Oxygen Species; Q, Quercetin; Q3BTPI, 3-(4-O-triphenylphosphoniumbutyl)quercetin iodide; QTA3BTPI, 3′,4′,5,7-tetra-O-acetyl-3-(4-O-triphenylphosphoniumbutyl)quercetin iodide; TMRM, Tetramethylrhodamine methyl ester; TPP, Triphenylphosphonium

* Corresponding author. CNR Institute of Neuroscience, c/o Department of Biomedical Sciences, Viale G. Colombo 3, 35121 Padova, Italy. Tel.: +39 0498276054; fax: +39 0498276049.
E-mail address: zoratti@bio.unipd.it (M. Zoratti).

0005-2728/$ – see front matter © 2009 Elsevier B.V. All rights reserved.
doi:10.1016/j.bbabio.2009.10.001

targeted quercetin derivatives, 3-(4-O-triphenylphosphoniumbutyl) quercetin iodide (Q3BTPI) and 3′,4′,5,7-tetra-O-acetyl-3-(4-O-triphenylphosphoniumbutyl)quercetin iodide (QTA3BTPI).

2. Materials and methods

2.1. Cells and mitochondria

HepG2 cells were grown in Dulbecco's Modified Eagle Medium (DMEM) (GIBCO) plus 10 mM HEPES buffer, 10% (v/v) fetal calf serum (Invitrogen), 100 U/mL penicillin G (Sigma), 0.1 mg/mL streptomycin (Sigma), 2 mM glutamine (GIBCO) and 1% nonessential amino acids (100× solution; GIBCO), in a humidified atmosphere of 5% CO_2 at 37 °C. Jurkat cells were grown in RPMI-1640 medium supplemented as above plus 50 μM β-mercaptoethanol. Rat liver mitochondria (RLM) were prepared by standard differential centrifugation procedures and obtained as a suspension in 0.25 M sucrose, 5 mM Hepes/K^+, pH 7.4.

2.2. TPP-sensitive electrode

The setup used to monitor the concentration of triphenylphosphonium-bearing compounds in solution was built in-house following published procedures [21,22]. In these electrodes the diffusion of the charged, permeant compound across a permeable polyvinylchloride (PVC) film gives rise to a half-cell potential logarithmically related to the concentration of the compound according to Nernst's law. The film is permeable because doped with tetraphenylborate anion, which acts as a carrier. Such an electrode will respond to all cations capable of diffusing into the PVC film as an ionic couple with tetraphenylborate, i.e., in practice, to triphenylphosphonium-comprising organic molecules. A calomel electrode was used as reference and the potentiometric output was directed to a strip chart recorder. The experiment illustrated in Fig. 1 was conducted at 20 °C.

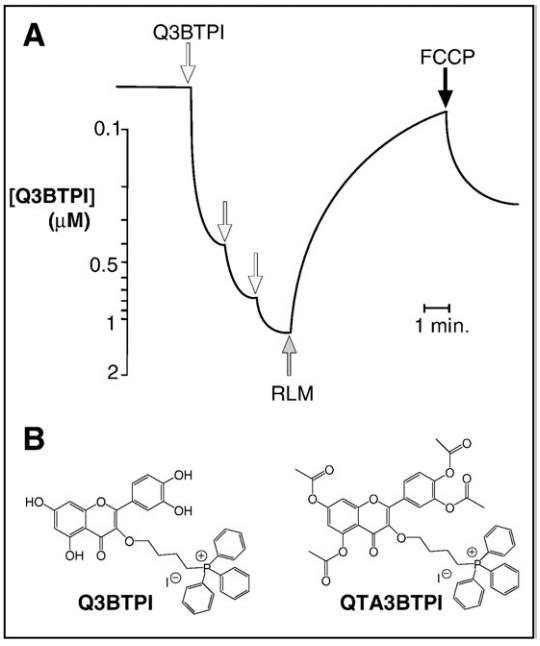

Fig. 1. (A) Accumulation of Q3BTPI by RLM. The response of a TPP-sensitive electrode is shown. Arrows indicate the addition of 0.4 μM Q3BTPI to standard medium. Addition of RLM (1 mg prot.mL^{-1}) causes an upward deflection of the trace since respiring mitochondria take up the positively charged compound, which also bind in part to mitochondrial components. Addition of FCCP causes release. (B) Chemical structures of Q3BTPI and QTA3BTPI.

2.3. Swelling and respiration assays

Preparation of RLM and swelling and respiration assays were carried out as described in [23]. The standard medium contained 250 mM sucrose, 10 mM Hepes/K^+, 5 mM succinate/K^+, 1.25 μM rotenone, 1 mM P_i/K^+, pH 7.4, supplemented with the desired concentration of $CaCl_2$. RLM were used at a concentration of 1 or 0.5 mg.prot.mL^{-1}. Direct determinations of the effects of Q3BTPI on respiration using a Clark electrode could not be carried out because Q3BTPI diffused through the semi-permeable Teflon membrane covering the working surface of the electrode (a cathode at which approximately −0.7 V are applied), and reacted there forming black polymeric products which rapidly gummed up the surface making the electrode unserviceable.

2.4. Fluorimetric assays of mitochondrial potential

Rhodamine 123 (75 nM) fluorescence was used to monitor the transmembrane potential of isolated RLM suspended (0.5 mg.prot. mL^{-1}) in standard medium in a stirred quartz cuvette placed in a Shimadzu RL-5000 spectrofluorimeter at R.T. Excitation was at 503 nm (3 nm slit), and fluorescence was collected at 523 nm (5 nm slit).

Tetramethylrhodamine methyl ester (TMRM; Invitrogen/Molecular Probes) staining of cells was used to monitor mitochondrial transmembrane potential in cultured cells. HepG2 cells were seeded onto 24-mm coverslips in 6-well plates and grown for about two days, avoiding confluence. Coverslips were mounted onto holders, exposed to 20 nM TMRM in DMEM or HBSS (in mM units: NaCl 136.9, KCl 5.36, $CaCl_2$ 1.26, $MgSO_4$ 0.81, KH_2PO_4 0.44, Na_2HPO_4 0.34, glucose 5.55, pH 7.4 with NaOH) for about 20 min, generally in the presence of 4 μM Cyclosporin H or 2 μM Cyclosporin A depending on the details of the experimental protocol, and washed twice. Cells were then covered with 1 mL of the desired medium and observed at room temperature. Images were acquired automatically at 1- or 2-min intervals, using an Olympus Biosystems apparatus comprising an Olympus IX71 microscope and MT20 light source, and processed with Cell$^{R©}$ software. Excitation was at 568 ± 25 nm and fluorescence was collected using a 585-nm longpass filter. Additions were performed by withdrawing 0.5 mL of incubation medium, adding the desired solute to this aliquot, mixing, and adding back the solution into the chamber at a peripheral point.

A Beckton Dickinson Canto II flow cytometer was used to monitor TMRM fluorescence of Jurkat cells. The cells were washed in HBSS, suspended in FACS buffer (135 mM NaCl, 10 mM Hepes, 5 mM $CaCl_2$, pH 7.4) at a density of 1.5×10^6/mL and loaded with 20 nM TMRM (37° C, 20 min). Cells were then diluted 1:5 in FACS buffer and divided into the desired number of identical aliquots. At time zero the desired compound was added, and data collected after the desired incubation times, exciting at 545 nm and measuring fluorescence at 585 nm. Data were analysed using the BD VISTA software. Experiments could be performed only with QTA3BTPI because Q3BTPI significantly altered the scatter parameters of a large fraction of the cells.

2.5. Superoxide production assays

Dihydroethidine (Invitrogen/Molecular Probes) assays were used as described in [23] to detect the production of $O_2^{\cdot-}$ in RLM suspensions. Superoxide generation in cells was followed using the mitochondriotropic probe MitoSOX Red® (Invitrogen/Molecular Probes) used as specified by the producer. Cells were incubated for 15 min with 1 or 2 μM MitoSOX Red® in HBSS, washed twice, covered with 1 mL HBSS, and placed on the microscope stage. Excitation was at 500–520 nm, and fluorescence was collected at λ>570 nm. Images were automatically acquired at 1 or 2 min intervals as above. These experiments could be conducted only with QTA3BTPI and 5 μM Q3BTPI, because 20 μM Q3BTPI apparently interacted with mitoSOX to

produce strongly fluorescent microaggregates giving rise to a "snow-storm" effect which masked any fluorescence increase.

FACS experiments with Jurkat cells were conducted as described for TMRM fluorescence determinations, loading with 1 μM MitoSOX Red®. Also in this case analyses could be performed only with QTA3BTPI.

2.6. QTA3BTPI stability in mitochondrial suspensions

QTA3BTPI was added to a 1 mg.prot.mL^{-1} suspension of RLM in standard medium to give a 20 μM solution. 100 μL samples were withdrawn, stabilised with 1 mM ascorbate and 0.06 M acetic acid, and mixed with an equal volume of acetone. After sonication the solids were separated by centrifugation. The supernatant was concentrated under N_2 and analysed. LC-ESI/MS analyses and mass spectra were performed with a 1100 Series Agilent Technologies system, equipped with binary pump (G1312A) and MSD SL Trap mass spectrometer (G2445D SL) with ESI source. Samples (20 μl) were injected onto a reversed phase column (Gemini C18, 3 μm, 150×4.6 mm i.d.; Phenomenex). Solvents A and B were H_2O containing 0.1% formic acid and CH_3CN, respectively. The gradient for B was as follows: 30% for 5 min, from 30% to 60% in 15 min, from 60% to 100% in 3 min; the flow rate was 0.7 mL/min. The eluate was monitored at 300 nm.

3. Results

To assess the effects of Q3BTPI and QTA3BTPI on isolated rat liver mitochondria we monitored three classical readouts of bioenergetics experiments: mitochondrial volume (as reflected by light scattering), transmembrane potential and oxygen consumption. These parameters, and their variation in response to pharmacological agents, vary to some extent from one preparation to the other. The direct comparisons presented in this paper are based on data obtained with the same preparation.

As an initial step we simply mixed the compounds with RLM suspended in an isotonic sucrose-based medium. Both QTA3BTPI [19] and Q3BTPI (Fig. 1) can be observed to accumulate into isolated mitochondria by monitoring their concentration with a TPP-responsive electrode. Note that Q3BTPI is only partially released upon uncoupling of the organelles indicating that much of the compound is actually bound. Polyphenols are well known to bind avidly to proteins, and the TPP moiety is also understood to participate in interactions with membranes and with macromolecules bearing negative charges (DNA). The group of Smith and Murphy has recently produced a quantitative study of the partition of mitoQ in cells: most of the compound was found to bind to cellular components [24]. Acetylation of the OH groups allows faster redistribution and less extensive binding of QTA3BTPI [19].

Fig. 2A illustrates the results of light-scattering experiments with Q3BTPI under these conditions ($N=3$). In this as well as in the other figures representative experiments are shown, utilising concentrations of the compounds producing a marked change of the readout parameter. Lower concentrations always had similar, but less evident, effects or produced variations too small for a reliable assessment. In the presence of 20 μM Q3BTPI (trace 1) swelling ensued which was not observed when no addition was made (trace 7, with oxygenation) or in the presence of 20 μM tetraphenylphosphonium chloride (trace 6). The latter induced only a much slower and lower-amplitude swelling, presumably due to the energy-driven uptake of the osmotically active solute since it was abolished by FCCP (not shown). The pseudo-absorbance decrease induced by Q3BTPI was in turn more modest than that associated with full-blown Ca^{2+}-induced permeability transition (trace 8), it was partly sensitive to Cyclosporin A (trace 2) and EGTA (trace 9), abolished by FCCP (trace 3) and it was interrupted by a sudden inversion (traces 1, 2). The latter was

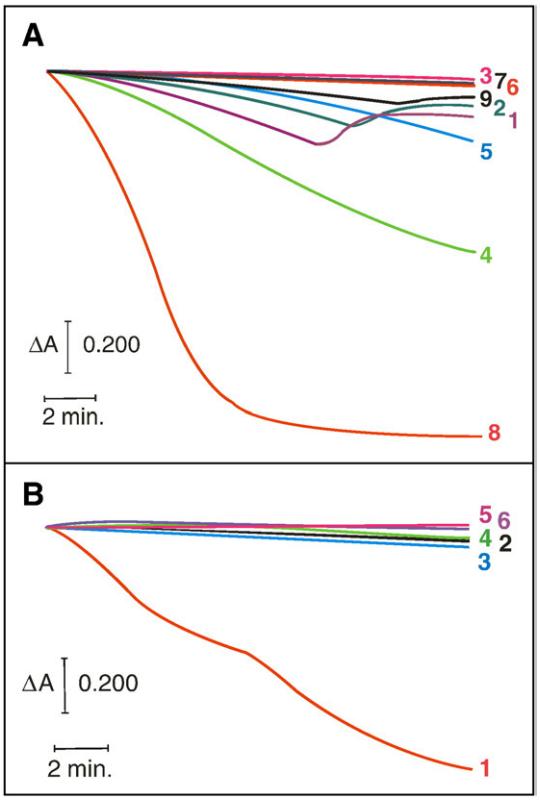

Fig. 2. Effects of Q3BTPI and QTA3BTPI on isolated rat liver mitochondria in the absence of added Ca^{2+}. Parallel light scattering experiments initiated by the addition of 1 mg.prot.mL^{-1} RLM to the cuvettes. Pseudo-absorbance was monitored at 540 nm. The medium contained: (A) traces 1–5 and trace 9: Q3BTPI 20 μM; traces 2,5: CsA 1 μM; trace 3: FCCP 1 μM; trace 6: $Ph_4P^+Cl^-$ 20 μM; trace 8: $CaCl_2$ 80 μM; trace 9: EGTA 100 μM; traces 4, 5, 7, 8: the incubation medium saturated with oxygen; (B) traces 1–3: QTA3BTPI 20 μM; trace 2: CsA 1 μM; trace 3: EGTA 100 μM; traces 4–6: Q 20 μM; trace 5: CsA 1 μM; trace 6: EGTA 100 μM.

associated with the near-exhaustion of the oxygen supply in the spectrophotometer cuvette, since saturating the suspension medium with oxygen beforehand delayed the phenomenon (traces 4, 5). This behaviour indicates that oxygen consumption was strongly enhanced by Q3BTPI. This could not be confirmed directly by measurements with a Clark electrode, because Q3BTPI reacted at the electrode surface producing a tarry substance which rapidly rendered the electrode useless. Oxygenation on the other hand increased the CsA-sensitive portion of the pseudo-absorbance decrease (compare traces 1, 2 vs. 4, 5), i.e., the rate of propagation of the permeability transition in the suspension, confirming that this phenomenon is mediated by oxidative events [23].

The acetylated derivative–QTA3BTPI–and quercetin affected swelling differently, as illustrated in Fig. 2B. In the absence of added Ca^{2+} quercetin in the 10–50 μM range had little effect (cf. trace 4 in Fig. 2B). QTA3BTPI on the other hand induced large amplitude swelling (trace 1) which was essentially abolished by both cyclosporin A and EGTA (traces 2 and 3), and can thus be attributed to the permeability transition taking place in the presence of "contaminating" Ca^{2+}.

These results suggested that both Q3BTPI and QTA3BTPI acted as inducers of the MPT in synergy with any Ca^{2+} present. In this capacity QTA3BTPI seemed to be more efficient than Q3BTPI (in Fig. 2 compare trace 1 minus trace 2 in panel B for QTA3BTPI vs. trace 1 minus trace 2 in panel A for Q3BTPI), which in turn was more efficient than quercetin itself (trace 4 minus trace 5 in panel B). These indications were confirmed by experiments performed in the presence of near-threshold [Ca^{2+}], i.e. of a concentration of Ca^{2+} sufficient for only a slowly-developing MPT-associated swelling in the absence of another

inducing agent (Fig. 3) ($N=31$). QTA3BTPI-induced swelling was always profoundly inhibited by CsA, at variance from that caused by Q3BTPI, which was only partially sensitive (in Fig. 3 compare trace 2 for QTA3BTPI + CsA with trace 4 for Q3BTPI + CsA). Thus, while QTA3BTPI is more efficient at inducing the MPT, Q3BTPI is more efficient at inducing CsA-insensitive swelling. These properties clearly must be related to the presence of free OH groups in Q3BTPI. Quercetin has been shown to induce the MPT via a metal ion-catalyzed oxidative process [23] and the same mechanism may be envisioned for the present compounds. In the presence of metal ions with multiple possible oxidation states (mainly $Fe^{2+/3+}$ and $Cu^{+/2+}$) polyphenols, especially if comprising a catechol moiety, may oxidize in chain reactions producing superoxide and hence H_2O_2. The latter can then undergo Fenton-type reactions producing more aggressive hydroxy and peroxy radicals [25,26]. Oxygen radicals, or, in general, oxidising conditions, are well known to favour the onset of the MPT by acting on key thiol residues [27–29].

MPT induction by QTA3BTPI was somewhat unexpected because the hydroxyls, the sites of oxidation in quercetin, are protected by acetylation. LC/MS analysis revealed that QTA3BTPI undergoes partial deacetylation, producing oxidisable species still capable of electrophoretic accumulation into energised mitochondria (Fig. 4). However over the time course of a swelling experiment essentially no Q3BTPI is produced: the main species found at 15 min still retain two or three of the original four acetyl groups.

The intervention of radicalic/oxidative processes in the onset of QTA3BTPI-induced MPT and, in part, of Q3BTPI-induced swelling was confirmed by the inhibition afforded by BHT + DTT (Fig. 5A) ($N=3$). In the case of quercetin, MPT induction was antagonised by Fe and Cu chelating agents [23], indicating the involvement of Fenton reactions catalysed by metallic species released by or associated with the mitochondria themselves. Selective chelators also affected Q3BTPI and Ca^{2+}-associated swelling (Fig. 5B) ($N=3$), reducing not only the CsA-sensitive component of the swelling curve, but also the CsA-insensitive one (compare traces 6 and 7 in Fig. 5B). This suggests that CsA-insensitive swelling is also largely mediated by ROS produced by metal-catalysed processes, presumably via aspecific membrane permeabilisation by lipoxidation. On the other hand in the case of QTA3BTPI this protective effect was practically absent (compare traces 1 and 2). This would be expected if in this case the relevant redox events took place mostly in the mitochondrial matrix, where QTA3BTPI accumulates. The matrix is inaccessible to BC and BF which are sulfonated (i.e., negatively charged) molecules.

QTA3BTPI is much less reactive than Q3BTPI at the Clark electrode surface, and its effects on respiration can therefore be assessed by

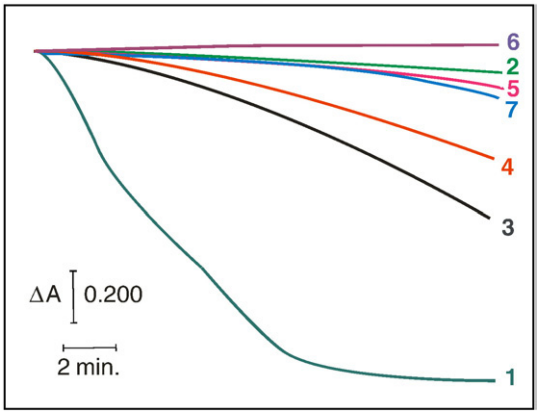

Fig. 3. Effects of Q, Q3BTPI and QTA3BTPI on isolated rat liver mitochondria in the presence of exogenous Ca^{2+}. Light scattering experiments analogous to those of Fig. 2. In all cases the medium was saturated with oxygen and contained $CaCl_2$ 50 μM plus: traces 1,2: QTA3BTPI 10 μM; trace 2: CsA 1 μM; traces 3,4: Q3BTPI 20 μM; trace 4: CsA 1 μM; traces 5, 6: Q 40 μM; trace 6: CsA 1 μM.

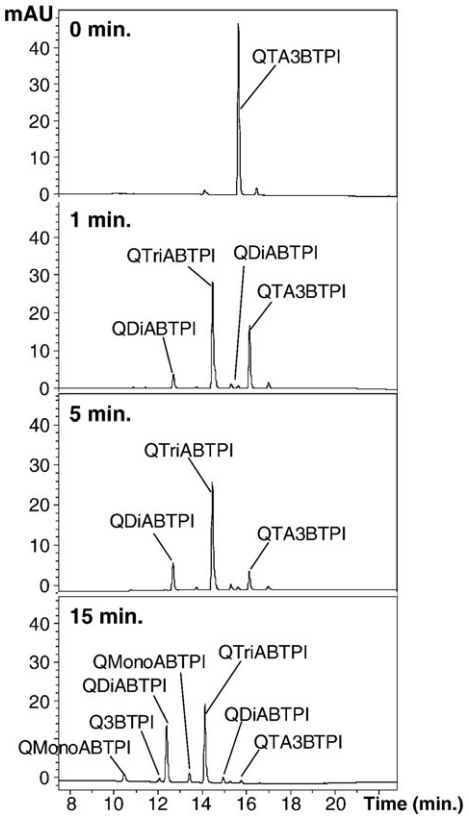

Fig. 4. Deacetylation of QTA3BTPI in the presence of RLM. HPLC chromatograms (300 nm) recorded after different incubation periods of QTA3BTPI with a RLM suspension (1 mg.prot.mL^{-1}). Peak identity was determined by ESI/MS analysis.

polarography. As expected, in the presence of Ca^{2+} its addition caused an acceleration of the rate of oxygen consumption which was blocked by CsA (not shown). An increase in respiratory rate normally implies "uncoupling" of the mitochondrial energy conversion process, which in turn, according to the chemiosmotic model, implies a decrease of the transmembrane electrochemical proton gradient ($\Delta\tilde{\mu}_H$). To verify whether such a decrease was taking place we used the fluorescent transmembrane potential ($\Delta\Psi$) indicator dye Rhodamine 123 (Rh123). In these experiments Rh123 was added to the suspension and equilibrated, so that some was always present outside mitochondria. The high (0.5 mg.prot./mL) density of the latter then insured that any dye released upon depolarisation could be rapidly taken up again upon repolarisation. Q3BTPI indeed induced a sustained recovery of Rh123 fluorescence, corresponding to a decrease of $\Delta\Psi$, when added to a suspension of RLM, also if no Ca^{2+} was added and CsA was present to block the MPT (Fig. 6A) ($N=3$). QTA3BTPI had an analogous depolarising effect (Fig. 6B). In the presence of CsA, however, the increase of Rh123 fluorescence was transient, suggesting a rapid depolarisation due to influx of the permeant cation followed by a slower repolarisation taking place on the time scale of a few minutes (Fig. 6C; $N=4$), as the compound was taken up and an equilibrium distribution was approached. Quercetin itself had little effect under the same conditions (not shown).

We then checked whether our compounds affected mitochondria inside cultured cells (Fig. 7). We followed the mitochondrial potential via TMRM fluorescence. In the experiments of Fig. 7A, representative of 37 separate ones under various conditions, HepG2 cells were loaded with TMRM in the presence of CsH (to inhibit MDR pumps; CsH, contrary to CsA, does not prevent the MPT) and then incubated in HBSS without any pharmacological agent. Under these conditions there was a background loss of TMRM fluorescence (plot "a"), which was hardly affected by the addition of 5 μM Q3BTPI (plot "b"), while

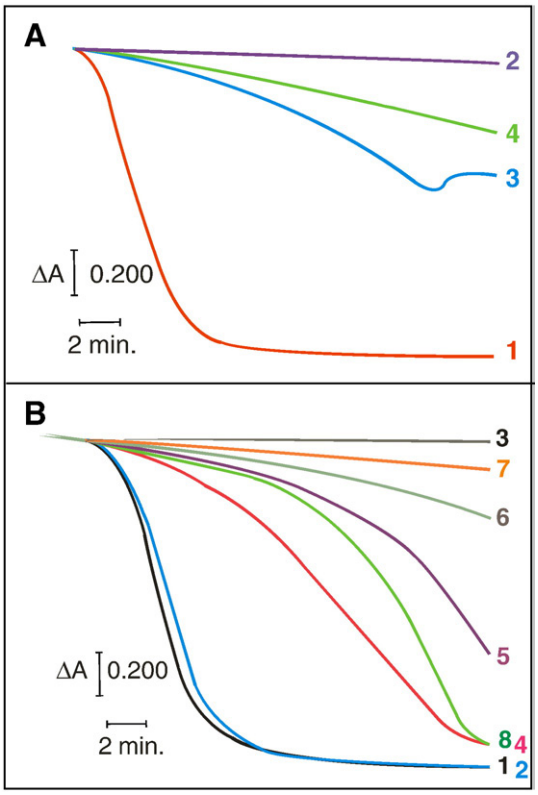

Fig. 5. Contribution of Fe and Cu ions and radical species to the induction of the mitochondrial permeability transition by Q3BTPI and QTA3BTPI. Light scattering experiments analogous to those in Figs 2 and 3. In all cases the medium was saturated with oxygen. (A) All traces: $CaCl_2$ 50 μM. Traces 1, 2: QTA3BTPI 10 μM; trace 2: BHT and DTT, 1 mM each; traces 3, 4: Q3BTPI 20 μM; trace 4: BHT and DTT, 1 mM each. (B) The medium contained $CaCl_2$ 40 μM plus: traces 1–3: QTA3BTPI 10 μM; trace 2: BF and BC, 10 μM each; trace 3: CsA 1 μM; traces 4–7: Q3BTPI 20 μM; trace 5: BF and BC, 10 μM each; trace 6: CsA 1 μM; trace 7: BF and BC, 10 μM each, and CsA 1 μM.

20 μM resulted in a modest acceleration (plot "c"). This sluggishness may be explainable in terms of the sequestration of a fraction of this compound by cellular structures.

QTA3BTPI is expected to bind less avidly, since its hydroxyls are capped, and it has been directly observed to accumulate into *in situ* mitochondria [19]. Accordingly, its addition induced a more pronounced but transient acceleration of the fluorescence decrease (plot "d"), which was not affected by either CsA or BHT + DTT (1 mM each) (not shown), ruling out the MPT as its origin. Fluorescence loss proceeded with kinetics comparable to those of QTA3BTPI uptake [19], suggesting that the two phenomena are correlated, i.e., the process may be ascribable to the depolarisation associated with uptake of a permeant cation. A protonophoric cycle by (partially) deacylated species may also intervene. The same type of behaviour by QTA3BTPI was observed when Jurkat cells were analysed by cytofluorimetry (Fig. 7B, C). In the case of Q3BTPI reliable data could not be obtained (see Materials and methods). In experiments with cells loss of TMRM fluorescence does not necessarily indicate an irreversible, permanent depolarisation of the mitochondria. Cells are pre-loaded with TMRM and then washed, so that no dye is present outside cells, a non-equilibrium situation. Indeed, TMRM slowly leaks out of cells under our control conditions. The cells face an extremely larger volume of incubation medium. Under these conditions, any TMRM lost because of a transient depolarisation would not be expected to be regained upon a subsequent recovery of the mitochondrial potential. Thus, fluorescence loss indicates depolarisation, but does not necessarily indicate by itself a *permanent* depolarisation or damage.

Quercetin induces the production of superoxide anion by isolated mitochondria as well as by cultured cells [23]. We could not obtain clear evidence of an analogous effect by Q3BTPI or QTA3BTPI on isolated mitochondria using HE or mitoSOX®. A reliable assessment of the effect of Q3BTPI on the response of MitoSOX® in HepG2 or Jurkat cells was made difficult by technical problems at 20 μM (see Materials and methods) and was not robust enough to reach definite conclusions at the 5 μM level. Addition of QTA3BTPI resulted instead in a fluorescence increase, which took place also in the presence of CsA (Fig. 8). In microscopy experiments an heterogeneity of cell behaviour was evident, as illustrated by the different increases of the fluorescence associated with two cells in the same field shown in Fig. 8A (plots "b" and "c").

4. Discussion

The results presented above plausibly identify the mechanisms responsible for the cytotoxicity of Q3BTPI and QTA3BTPI. They have been obtained *in vitro*, with relatively high concentrations, but we believe they are relevant also for an eventual *in vivo* utilisation of the compounds, since much the same mechanisms and requirements would be expected to apply. Polyphenols *per se* have rather poor bioavailability, and when administered in foods or beverages they are unlikely to reach μM-range concentrations in blood and organs (except as phase II conjugates). Here we are however considering not the natural compounds, but their derivatives, which may be considered as drugs, and administered in various ways. Pharmacological delivery methods can be expected to result in much higher levels, at least locally.

We rationalise the behaviour of Q3BTPI vs. isolated mitochondria in terms of three major concomitant processes: uncoupling of the mitochondria by Q3BTPI acting as a protonophore (Fig. 9), MPT induction–involving Ca^{2+} and ROS in analogy to the process induced by quercetin itself under similar conditions [23]–and CsA-insensitive permeabilisation of the IMM, with consequent swelling, due to the action of ROS on membrane lipids. The uncoupling effect of Q3BTPI

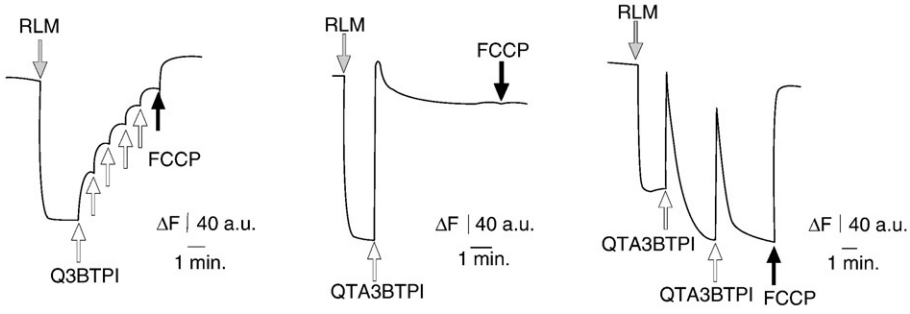

Fig. 6. Effects of Q3BTPI and QTA3BTPI on mitochondrial membrane potential. Variations of Rhodamine 123 fluorescence upon additions of: (A) Q3BTPI (each arrow represents a 10 μM addition); (B, C) QTA3BTPI (each arrow represents a 20 μM addition). In A and C, CsA 1 μM was present during the experiment.

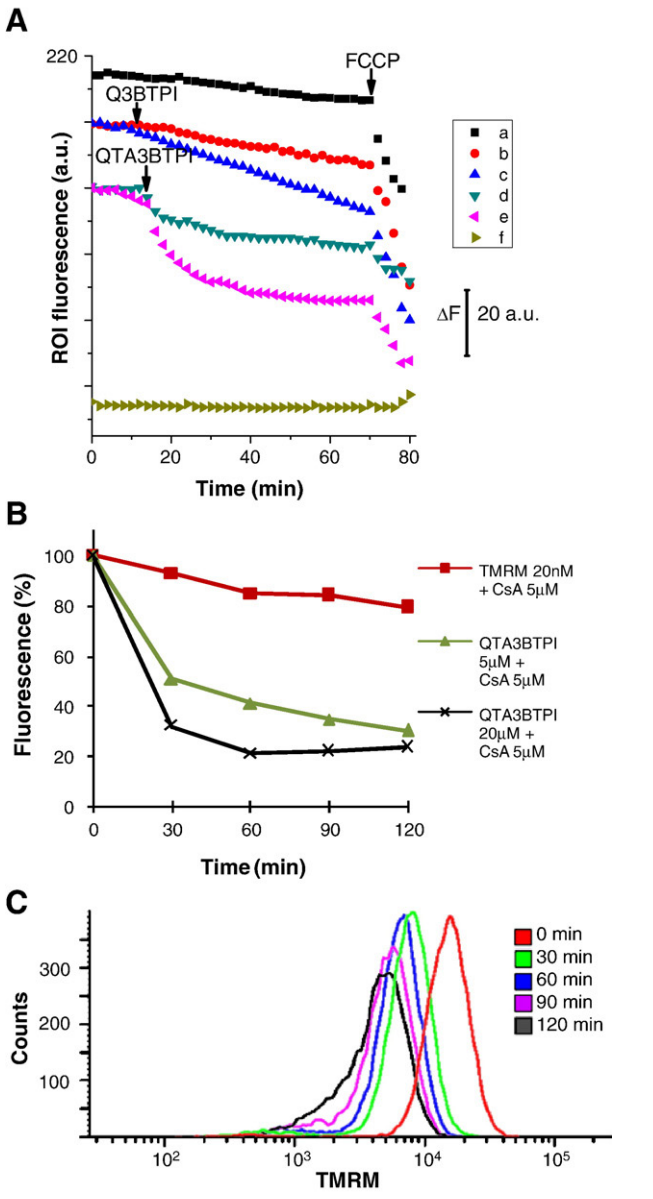

Fig. 7. Mitochondrial membrane potential in cells exposed to Q3BTPI and QTA3BTPI, monitored using TMRM. (A) Representative fluorescence microscopy experiments with TMRM-loaded HepG2 cells. Computer-generated plots of the fluorescence emitted by the field areas (Regions Of Interest, ROI) coinciding with one cell or a portion of background (f). Images were acquired every 60 s. Plot "a" represents a control experiment without addition. Plot "b": Q3BTPI 5 μM; plot "c": Q3BTPI 20 μM; plot "d": QTA3BTPI 5 μM; plot "e": QTA3BTPI 20 μM. Compound additions are indicated by arrows. Plots have been shifted along the ordinate axis for clarity. See Materials and methods for details. (B) Representative FACS experiments with 0 (red; control), 5 (green) or 20 μM (black) QTA3BTPI additions. The experiment was conducted in the presence of 5 μM CsA. Plotted are the normalised median values of histograms such as those shown in panel C. The median of the histogram recorded immediately after the addition of QTA3BTPI was set as 100%. (C) The set of histograms obtained in the experiment with 5 μM QTA3BTPI shown in panel B is shown as an example.

can be explained as follows: Q3BTPI exists in solution as a mixture of instantaneously fully protonated (i.e., positively charged due to the TPP group) and deprotonated species (the first pKa of quercetin is close to 7 [30–32]). The mitochondrial $\Delta\Psi$ will drive the uptake of fully protonated molecules, the chemical gradient between the matrix and the suspension medium will drive the efflux of the unprotonated, zwitterionic specie. A $\Delta\Psi$-decreasing, respiration-stimulating protonophoric futile cycle will thus be generated. Flavonoids have already been identified as potential uncouplers [33], but the presence of the membrane-permeating positive charge enhances this characteristic: quercetin itself is not active as an uncoupler at concentrations below 1 mM [33], while Q3BTPI uncouples in the μM range. Active uptake of Q3BTPI by energised mitochondria is therefore self-limiting.

Direct comparison shows that both QTA3BTPI and Q3BTPI are more efficient MPT co-inducers than quercetin (Fig. 3) in RLM. Since these compounds are accumulated inside suspended mitochondria, this indicates that induction can be mediated by phenomena taking place in the matrix. The higher efficiency is then presumably accounted for by the higher concentration of inducer on the matrix side of the inner mitochondrial membrane (IMM) (in comparison with an analogous experiment with quercetin). While the two mitochondriotropic compounds are better inducers than quercetin,

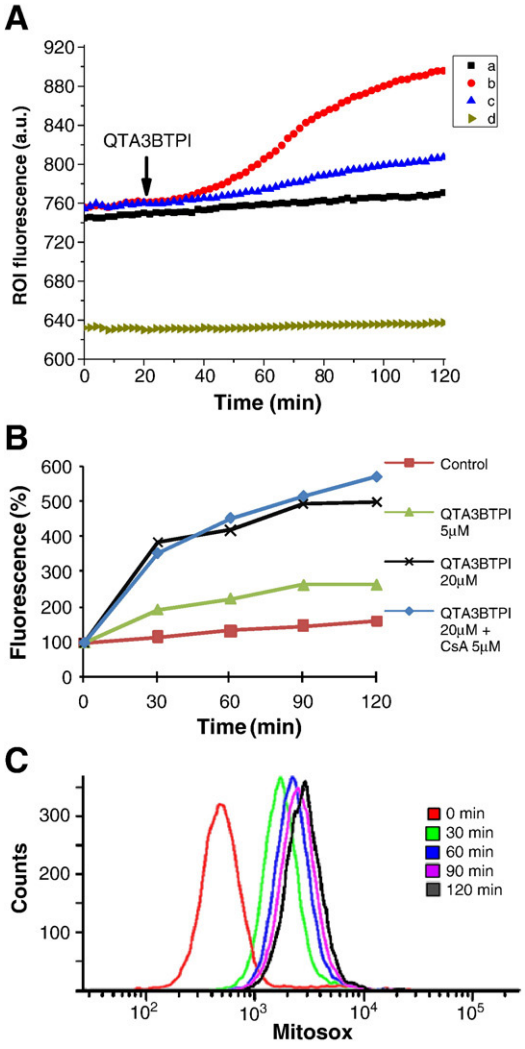

Fig. 8. Superoxide production in cells exposed to QTA3BTPI, monitored using MitoSOX Red®. (A) Representative fluorescence microscopy experiments with MitoSOX Red®-loaded HepG2 cells. A computer-generated plot of the fluorescence emitted by field areas (Regions Of Interest, ROI) coinciding with a cell (a–c) or a portion of background (d). Images were acquired every 2 min. Plot "a" presents the fluorescence associated with a cell in a separate control experiment without additions. 20 μM QTA3BTPI was added, when indicated, in plots "b" and "c", which report the fluorescence associated with two cells in the same field (plot "d" also comes from the same experiment). See Materials and methods for details. (B) Representative FACS experiments with 0 (red; control), 5 (green) or 20 μM (black) QTA3BTPI additions. The graph plotted in blue refer to a parallel experiment with 20 μM QTA3BTPI in the presence of 5 μM CsA. Plotted are the normalised median values of histograms such as those shown in panel C. The median of the histogram recorded immediately after the addition of QTA3BTPI was set as 100%. (C) The set of histograms obtained in the experiment with 20 μM QTA3BTPI in the presence of CsA shown in panel B (blue plot) is shown as an example.

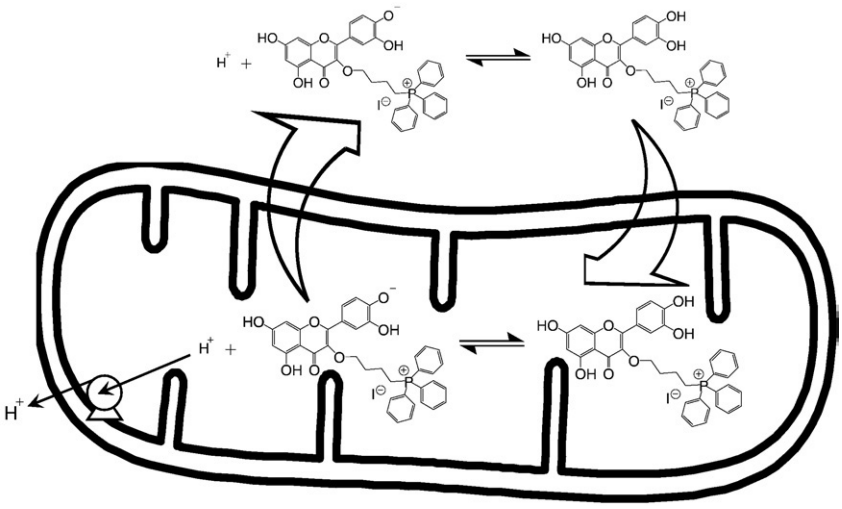

Fig. 9. An illustration of how Q3BTPI may act as a protonophore and uncoupler. See text for details.

the difference is less marked than might have been expected. In the case of Q3BTPI this may be explained by uncoupling, which limits matrix accumulation of both Ca^{2+} and inducer. QTA3BTPI is expected to be less effective than quercetin or Q3BTPI, at parity of concentration, because its hydroxyls are at least initially blocked (see Fig. 4).

The observations on cultured cells differ in some respects from those with isolated mitochondria, indicating that the MPT is much less readily induced in *in situ* mitochondria. This is coherent with the low concentration of Ca^{2+} and of transition metals–the two factors involved in MPT induction with isolated RLM–in the cytoplasm. At least in the case of QTA3BTPI, MPT-independent (because CsA-insensitive) production of superoxide and some loss of $\Delta\Psi$ takes place. Other mitochondriotropic polyphenols may well behave differently, depending on their physico-chemical properties, but compounds of this class are in any case to be studied with care: it is not clear that *in vivo* they would behave only as beneficial antioxidants and ROS quenchers. The results of this investigation may be taken into consideration for the design of other mitochondriotropic compounds: features conferring protonophoric/uncoupling properties will best be avoided if the intention is to produce a cell-saving anti-oxidant molecule, and may conversely be desirable if a candidate for chemotherapeutic applications is desired. Usefulness in oncology may also be maximised by taking into account the findings that cancer cells have elevated levels of copper ions [34] and of oxidative stress [35]. On the other hand mild uncoupling of mitochondria is proposed to have potentially beneficial effects, such as mimicking life-extending caloric restriction (e.g.: [36,37]) and protecting neurons against excitotoxicity (e.g.: [38]). Thus, a less readily oxidisable polyphenol derivative with mild uncoupling activity may also find applications.

Literature reports suggest that concentration, or dosage, may well be an important parameter determining the overall effect of a (mitochondriotropic) polyphenol. For example, EpiGalloCatechin-Gallate (EGCG) may have anti-oxidant and "cell-protective" effects at low dosages (<μM), and pro-oxidant, cytotoxic effects at higher levels [39]. MitoQ, the best studied mitochondriotropic antioxidant, changes from an anti-oxidant to a pro-oxidant behaviour over a relatively small concentration range ([5] and references therein). Low doses of mitochondria-targeted plastoquinone derivatives reportedly exert very beneficial effects *in vivo* [5]. It remains to be seen whether the present compounds may display divergent effects at very low concentration, and whether there may be relatively sharp thresholds for these hypothetical different activities. It also remains to be seen what concentrations may be attained in the organs of laboratory animals, and by what means. Furthermore, as mentioned, the bioactivity of polyphenols is not limited to redox effects. The investigation of the activity of mitochondriotropic polyphenols *in vivo* will need therefore to consider several "readout" parameters, the most important obviously being the impact on physiological or pathological conditions of interest.

Acknowledgments

We thank I. Szabò and V. Petronilli for useful discussions, P. Bernardi's group and F. Zoccarato for access to instrumentation and instructions, U. De Marchi for preliminary experiments, M. Mancon for technical help. This work was supported in part by the Italian Foundation for Basic Research (FIRB), by the Italian Association for Cancer Research (AIRC) and by the University of Padova (Progetto d'Ateneo 2008 to S.G. and a post-doctoral fellowship to L.B.).

References

[1] K.C. Kregel, H.J. Zhang, An integrated view of oxidative stress in aging: basic mechanisms, functional effects, and pathological considerations, Am. J. Physiol. Integr. Comp. Physiol. 292 (2007) R18–R36.
[2] M. Valko, D. Leibfritz, J. Moncol, M.T. Cronin, M. Mazur, J. Telser, Free radicals and antioxidants in normal physiological functions and human disease, Int. J. Biochem. Cell Biol. 39 (2007) 44–84.
[3] A. Carpi, R. Menabò, N. Kaludercic, P. Pelicci, F. Di Lisa, M. Giorgio, The cardioprotective effects elicited by p66(Shc) ablation demonstrate the crucial role of mitochondrial ROS formation in ischemia/reperfusion injury, Biochim. Biophys. Acta 1787 (2009) 774–780.
[4] H. Du, S.S. Yan, Mitochondrial permeability transition pore in Alzheimer's disease: Cyclophilin D and amyloid beta, Biochim. Biophys. Acta 1802 (2010) 198–204.
[5] V.P. Skulachev, V.N. Anisimov, Y.N. Antonenko, L.E. Bakeeva, B.V. Chernyak, V.P. Erichev, O.F. Filenko, N.I. Kalinina, V.I. Kapelko, N.G. Kolosova, B.P. Kopnin, G.A. Korshunova, M.R. Lichinitser, L.A. Obukhova, E.G. Pasyukova, O.I. Pisarenko, V.A. Roginsky, E.K. Ruuge, I.I. Senin, I.I. Severina, M.V. Skulachev, I.M. Spivak, V.N. Tashlitsky, V.A. Tkachuk, M.Y. Vyssokikh, L.S. Yaguzhinsky, D.B. Zorov, An attempt to prevent senescence: a mitochondrial approach, Biochim. Biophys. Acta. 1787 (2009) 437–461.
[6] P. Bernardi, A. Krauskopf, E. Basso, V. Petronilli, E. Blachly-Dyson, F. Di Lisa, M.A. Forte, The mitochondrial permeability transition from *in vitro* artifact to disease target, FEBS J. 273 (2006) 2077–2099.
[7] A. Rasola, P. Bernardi, The mitochondrial permeability transition pore and its involvement in cell death and in disease pathogenesis, Apoptosis 12 (2007) 815–833.
[8] A.P. Halestrap, What is the mitochondrial permeability transition pore? J. Mol. Cell. Cardiol. 46 (2009) 821–831.
[9] J.L. Zweier, M.A. Talukder, The role of oxidants and free radicals in reperfusion injury, Cardiovasc. Res. 70 (2006) 181–190.
[10] V. Petronilli, J. Sileikyte, A. Zulian, F. Dabbeni-Sala, G. Jori, S. Gobbo, G. Tognon, P. Nikolov, P. Bernardi, F. Ricchelli, Switch from inhibition to activation of the mitochondrial permeability transition during hematoporphyrin-mediated photo-oxidative stress. Unmasking pore-regulating external thiols, Biochim Biophys. Acta 1787 (2009) 897–904.
[11] V. Weissig, Targeted drug delivery to mammalian mitochondria in living cells, Expert Opin Drug Deliv. 2 (2005) 89–102.

[12] M.P. Murphy, R.A. Smith, Targeting antioxidants to mitochondria by conjugation to lipophilic cations, Annu. Rev. Pharmacol. Toxicol. 47 (2007) 629–656.
[13] A.T. Hoye, J.E. Davoren, P. Wipf, M.P. Fink, V.E. Kagan, Targeting mitochondria, Acc. Chem. Res. 41 (2008) 87–97.
[14] M.P. Murphy, Targeting lipophilic cations to mitochondria, Biochim. Biophys. Acta 1777 (2008) 1028–1031.
[15] H.H. Szeto, Development of mitochondria-targeted aromatic-cationic peptides for neurodegenerative diseases, Ann. N.Y. Acad. Sci. 1147 (2008) 112–121.
[16] H.H. Szeto, Mitochondria-targeted cytoprotective peptides for ischemia-reperfusion injury, Antiox. Redox Signal. 10 (2008) 601–619.
[17] T.A. Prime, F.H. Blaikie, C. Evans, S.M. Nadtochiy, A.M. James, C.C. Dahm, D.A. Vitturi, R.P. Patel, C.R. Hiley, I. Abakumova, R. Requejo, E.T. Chouchani, T.R. Hurd, J.F. Garvey, C.T. Taylor, P.S. Brookes, R.A. Smith, M.P. Murphy, A mitochondria-targeted S-nitrosothiol modulates respiration, nitrosates thiols, and protects against ischemia-reperfusion injury, Proc. Natl. Acad. Sci. USA 106 (2009) 10764–10769.
[18] J. Ripcke, K. Zarse, M. Ristow, M. Birringer, Small-molecule targeting of the mitochondrial compartment with an endogenously cleaved reversible tag, Chembiochem 10 (2009) 1689–1696.
[19] A. Mattarei, L. Biasutto, E. Marotta, U. De Marchi, N. Sassi, S. Garbisa, M. Zoratti, C. Paradisi, A mitochondriotropic derivative of quercetin: a strategy to increase the effectiveness of polyphenols, Chembiochem 9 (2008) 2633–2642.
[20] L. Biasutto, A. Mattarei, E. Marotta, A. Bradaschia, N. Sassi, S. Garbisa, M. Zoratti, C. Paradisi, Development of mitochondria-targeted derivatives of resveratrol, Bioorg. Med. Chem. Lett. 18 (2008) 5594–5597.
[21] N. Kamo, M. Muratsugu, R. Hongoh, Y. Kobatake, Membrane potential of mitochondria measured with an electrode sensitive to tetraphenyl phosphonium and relationship between proton electrochemical potential and phosphorylation potential in steady state, J. Membr. Biol. 49 (1979) 105–121.
[22] M. Zoratti, M. Favaron, D. Pietrobon, V. Petronilli, Nigericin-induced transient changes in rat-liver mitochondria, Biochim. Biophys. Acta. 767 (1984) 231–239.
[23] U. De Marchi, L. Biasutto, S. Garbisa, A. Toninello, M. Zoratti, Quercetin can act either as an inhibitor or an inducer of the mitochondrial permeability transition pore: A demonstration of the ambivalent redox character of polyphenols, Biochim. Biophys. Acta. 1787 (2009) 1425–1432.
[24] M.F. Ross, T.A. Prime, I. Abakumova, A.M. James, C.M. Porteous, R.A. Smith, M.P. Murphy, Rapid and extensive uptake and activation of hydrophobic triphenylphosphonium cations within cells, Biochem. J. 411 (2008) 633–645.
[25] Y. Sakihama, M.F. Cohen, S.C. Grace, H. Yamasaki, Plant phenolic antioxidant and prooxidant activities: phenolics-induced oxidative damage mediated by metals in plants, Toxicology 177 (2002) 67–80.
[26] U. Shamim, S. Hanif, M.F. Ullah, A.S. Azmi, S.H. Bhat, S.M. Hadi, Plant polyphenols mobilize nuclear copper in human peripheral lymphocytes leading to oxidatively generated DNA breakage: implications for an anticancer mechanism, Free Radic. Res. 42 (2008) 764–772.
[27] V. Petronilli, P. Costantini, L. Scorrano, R. Colonna, S. Passamonti, P. Bernardi, The voltage sensor of the mitochondrial permeability transition pore is tuned by the oxidation-reduction state of vicinal thiols. Increase of the gating potential by oxidants and its reversal by reducing agents, J. Biol. Chem. 269 (1994) 16638–16642.
[28] P. Costantini, B.V. Chernyak, V. Petronilli, P. Bernardi, Modulation of the mitochondrial permeability transition pore by pyridine nucleotides and dithiol oxidation at two separate sites, J. Biol. Chem. 271 (1996) 6746–67451.
[29] P. Costantini, R. Colonna, P. Bernardi, Induction of the mitochondrial permeability transition by N-ethylmaleimide depends on secondary oxidation of critical thiol groups. Potentiation by copper-ortho-phenanthroline without dimerization of the adenine nucleotide translocase, Biochim. Biophys. Acta 1365 (1998) 385–392.
[30] S.V. Jovanovic, S. Steenken, M. Tosic, B. Marjanovic, M.G. Simic, Flavonoids as antioxidants, J. Am. Chem. Soc 116 (1994) 4846–4851.
[31] N. Sauerwald, M. Schwenk, J. Polster, E. Bengsch, Spectrophotometric pK determination of daphnetin, chlorogenic acid and quercetin, Z. Naturforsch. 53b (1998) 315–321.
[32] K. Lemanska, H. Szymusiak, B. Tyrakowska, R. Zielinski, A.E.M.F. Soffers, I.M.C. M. Rietjens, The influence of pH on antioxidant properties and the mechanism of antioxidant action of hydroxyflavones, Free Rad. Biol. Med. 31 (2001) 869–881.
[33] C. van Dijk, A.J. Driessen, K. Recourt, The uncoupling efficiency and affinity of flavonoids for vesicles, Biochem. Pharmacol. 60 (2000) 1593–1600.
[34] A. Gupte, R.J. Mumper, Elevated copper and oxidative stress in cancer cells as a target for cancer treatment, Cancer Treat. Rev. 35 (2009) 32–46.
[35] H. Pelicano, D. Carney, P. Huang, ROS stress in cancer cells and therapeutic implications, Drug Resist. Updat. 7 (2004) 97–110.
[36] C.E. Amara, E.G. Shankland, S.A. Jubrias, D.J. Marcinek, M.J. Kushmerick, K.E. Conley, Mild mitochondrial uncoupling impacts cellular aging in human muscles *in vivo*, Proc. Natl. Acad. Sci. U.S.A. 104 (2007) 1057–1062.
[37] C.C. Caldeira da Silva, F.M. Cerqueira, L.F. Barbosa, M.H. Medeiros, A.J. Kowaltowski, Mild mitochondrial uncoupling in mice affects energy metabolism, redox balance and longevity, Aging Cell 7 (2008) 552–560.
[38] D. Liu, M. Pitta, M.P. Mattson, Preventing NAD(+) depletion protects neurons against excitotoxicity: bioenergetic effects of mild mitochondrial uncoupling and caloric restriction, Ann. N.Y. Acad. Sci. 1147 (2008) 275–282.
[39] S. Mandel, O. Weinreb, T. Amit, M.B. Youdim, Cell signaling pathways in the neuroprotective actions of the green tea polyphenol (-)-epigallocatechin-3-gallate: implications for neurodegenerative diseases, J. Neurochem. 88 (2004) 1555–1569.